JAERI 1346

JAERI 1346

JP0550008

Molecular Dynamics Simulation Studies of Radiation Damaged DNA Molecules and Repair Enzymes

December 2004

日 本 原 子 力 研 究 所

Japan Atomic Energy Research Institute

JAERIレポートは，日本原子力研究所が研究成果編集委員会の審査を経て不定期に公刊している研究報告書です。

入手の問合わせは，日本原子力研究所研究情報部研究情報課（〒319-1195　茨城県那珂郡東海村）あて，お申し込み下さい。なお，このほかに財団法人原子力弘済会資料センター（〒319-1195　茨城県那珂郡東海村日本原子力研究所内）で複写による実費頒布をおこなっております。

JAERI reports are reviewed by the Board of Editors and issued irregularly.

Inquiries about availability of the reports should be addressed to Research Information Division, Department of Intellectual Resources, Japan Atomic Energy Research Institute, Tokai-mura, Naka-gun, Ibaraki-ken, 319-1195, Japan.

編集兼発行　　日本原子力研究所

Molecular Dynamics Simulation Studies of Radiation Damaged DNA Molecules and Repair Enzymes

Miroslav PINAK

Department of Health Physics
Tokai Research Establishment
Japan Atomic Energy Research Institute
Tokai-mura, Naka-gun, Ibaraki-ken

(Received March 7, 2003)

Abstract

Molecular dynamics (MD) studies on several radiation damages to DNA and their recognition by repair enzymes are introduced in order to describe the stepwise description of molecular process observed at radiation lesion sites. MD studies were performed on pyrimidine (thymine dimer, thymine glycol) and purine (8-oxoguanine) lesions using an MD simulation code AMBER 5.0. The force field was modified for each lesion. In all cases the significant structural changes in the DNA double helical structure were observed; a) the breaking of hydrogen bond network between complementary bases and resulting opening of the double helix (8-oxoguanine); b) the sharp bending of the DNA helix centered at the lesion site (thymine dimer, thymine glycol); and c) the flipping-out base on the strand complementary to the lesion (8-oxoguanine). These changes were related to the overall collapsing double helical structure around the lesion and might facilitate the docking of the repair enzyme into the DNA and formation of DNA-enzyme complex. In addition to the structural changes, at lesion sites there were found electrostatic interaction energy values different from those at native sites (thymine dimer –10 kcal/mol, thymine glycol –26 kcal/mol, 8-oxoguanine –48 kcal/mol). These values of electrostatic energy may discriminate lesion from values at native sites (thymine 0 kcal/mol, guanine –37 kcal/mol) and enable a repair enzyme to recognize a lesion during scanning DNA surface. The observed specific structural conformation and energetic properties at the lesions sites are factors that guide a repair enzyme to discriminate lesions from non-damaged native DNA segments.

Keywords: Radiation, DNA Damage, Molecular Dynamics, Radiation Risk

放射線損傷DNAと修復酵素の分子動力学シミュレーション

日本原子力研究所東海研究所保健物理部
Miroslav PINAK

(2003年3月7日受理)

要旨

放射線により損傷をうけたDNAの分子レベルにおける経時的変化を調べるために、数種類の代表的DNA損傷を対象として修復酵素による損傷認識過程の分子動力学シミュレーションを利用した研究を行った。ピリミジン塩基の損傷としてチミンダイマーとチミングリコール、プリン塩基の損傷として8-オキソグアニンを取り上げ、AMBER 5.0を用いたシミュレーションを行った。シミュレーションのための力場は損傷の種類毎に修正を加えた。全てのケースでDNA二重らせん構造の重大な構造変化が観察された。それらはa) 相補的な塩基との水素結合ネットワークの破壊による二重らせんの分離(8-オキソグアニン)、b) 損傷部位を中心としたDNAの折れ曲り(チミンダイマー、チミングリコール)、c) 相補的な塩基のDNA外へのフリッピングアウト(8-オキソグアニン)に大別される。これらの変化によりDNA二重らせん構造の全体的な崩壊が起り、その結果として修復酵素のDNAへの結合と複合体の形成が容易になることが示唆された。構造の変化に加えて、損傷部位において特異的な静電エネルギーが観察された(チミンダイマー:-10 kcal/mol、チミングリコール:-26 kcal/mol、8-オキソグアニン:-48 kcal/mol)。損傷がない場合の静電エネルギー(チミン:0 kcal/mol、グアニン:-37 kcal/mol)との違いを感知して、修復酵素はDNA表面をスキャンしている間に損傷を認識すると考えられる。損傷のあるDNAと損傷のないDNAとを修復酵素が区別するのに、これらの構造及びエネルギーの変化が重要な因子であることがわかった。

東海研究所:〒319-1195 茨城県東海村白方白根2-4

Contents

目次

Figure and table captions

1. Introduction

Ionizing radiation damages DNA and causes mutation and chromosomal changes in cells and in organisms [1]. A certain type of damages to DNA can lead to cell transformation or to cell death. Radiation as well as other chemical agents may damage DNA molecules several ways, directly or indirectly by interactions with DNA itself or with its environment. Some damages caused by ionizing radiation are chemically similar to a damage that occurs naturally in the cell: this "spontaneous" damage arises from the thermal instability of DNA as well as from the endogenous and enzymatic processes. Several metabolic pathways generate oxidative radicals within the cells, and these radicals can attack DNA to give both DNA damage and breakage [2]. DNA molecule, as the repository of genetic information and blueprint operation of the individual cell, is a primary target of the active oxidative products [3].

Considering these important features, it can be concluded that nearly all DNA damages are harmful. Therefore it is essential to reduce this damage to a tolerable level. The importance and the complexity of a DNA repair can be seen from the facts that:

a) DNA is the only biomolecule that is specifically repaired, while all the others are replaced;
b) more that 100 genes participate in various aspects of DNA repair, even in organisms with very small genomes [4].

Cancer is caused by mutations. In most cases, the "genetic instability" (elevated mutation rate) is required to permit accumulation of sufficient mutations to generate cancer during a human lifetime. DNA repair mechanisms promote genomic stability and prevent cancer. Many, perhaps most, cancers are thus at least partially attributable to defects in DNA repair [5].

In order to ensure correct cell proliferation and to eliminate potential mutagenic cells the functioning of repair enzymes removing the damaged DNA parts is very important. Several nucleotide sequences of specific DNA binding sites that are involved in gene regulation have been described, suggesting an existence of a code for recognition between DNA regulatory and repair enzymes and DNA sites [6, 7, 8, 9]. Considerable information regarding enzyme/DNA interaction has been gained from biological experiments. In several of these systems, both prokaryotes and eukaryotes, a DNA recognition α helix within the DNA binding domain has been observed [10, 11]. It is known that sequence specific enzymes' DNA binding by repair and regulatory enzymes occurs as a result of multistage hydrogen bonding and van der Waals interactions between DNA recognition amino acids of enzyme and nucleotides of DNA. However, the underlying mechanisms by which enzymes recognize specific or damaged sites on DNA are subject of debate [12, 13].

In the present paper, there are reported the results of several lesioned DNA molecules examined with respect to the enzyme/DNA interactions between amino acids and nucleotides. The method used was molecular dynamics (MD) simulation. Where available, the simulation data were compared with experimental (X-ray crystallography and NMR measurements) results. In the center of interest were oxidative and radiation damages to DNA base: 8-oxoguanine, thymine dimmer and thymine glycol and their potential impact on the DNA structure. Particularly electrostatic interaction energies were calculated. These interactions between DNA and enzyme may induce breakage of Watson-Crick nucleotide base pairing hydrogen bonds, further resulting in bending of the DNA, strand elongation and its unwinding. The formation of stable DNA-enzyme complex was also studied as an onset of repair process.

2. Molecular Dynamics Studies and Radiation Risk

Estimation of radiation risk to the organisms is primarily based on the epidemiological studies. These studies are mostly relevant for the high doses and dose rates and lack sufficient information at low doses, which are more relevant to human exposure to radiation. Extrapolation of high doses results to low doses region requires a detailed understanding of the mechanisms by which radiation induces cell mutations, cancer and other forms of genetic disorders. The biochemical and biological mechanisms of the cell response to the radiation and oxidative damages are controlled by a specific set of genes that encodes enzymes catalyzing cellular response to radiation damage. These enzymes attempt to repair the damage when it occurs.

Numbers of human genes encoding enzymes involved in repair process of DNA have been already discovered (e.g. hRAD51, XRCC4, hRAD52, hREV3, hNTH, hOGG1, etc.). These enzymes are involved in DNA repair via several pathways and are functioning in certain phases of the complex repair process. For the study of qualification of radiation risk, it is necessary to determine the specific pathways and features that are typical for DNA damages originated by radiation. In addition, the quantification of radiation risk would involve the study on relative efficiency of the repair processes in respect to the increased incidence of DNA damages above the endogenous level.

The followings are samples of several human disorders originated by radiation characterized by defects in DNA repair.

a) Patients with xeroderma pigmentosum (XP) have clinical sun sensitivity, extensive freckle-like lesions in sun exposed, increase in developing of skin cancer (basal cell carcinoma, squamos cell carcinoma and melanom). All XP cells have been detected to be deficient in DNA repair.

b) Patients with Cockayne syndrome (CS) have increased sun sensitivity, short statue and progressive neurological degeneration. In contrary to the xeroderma pigmentosum, Cockayne syndrome does not result in cancer-proneness. Cultured cells from CS patients have defective DNA repair.
c) Patients with trichodiostrophy have short statue, mental retardation and brittle hair. Their cells have also defective DNA repair.

All the above named disorders have similar DNA repair pathways at the molecular level: base and/or nucleotide excision repair. Specifically, isolated DNA base damages are removed by a base excision repair pathway while bulky damages are repaired by a nucleotide repair pathway in which a damaged segment of DNA strand is removed. Detailed descriptions of DNA radiation damages' repair pathways can be found elsewhere [14]. An excision repair pathway consists of following steps with several enzymes acting in each of them:

1. DNA damage recognition; Specific repair enzymes specifically search for and bind DNA lesions, and/or attract other repair enzymes to the damaged site.
2. DNA helix opening; Repair enzymes unwind the DNA double helix around the lesion.
3. Dual incision; An enzyme cuts the damaged DNA strand on opposite sides of the lesion.
4. Excision; A damaged DNA fragment containing the lesion is removed.
5. Gap-filling; The remaining gap is filled in polymerization and ligation.

Complexity of these repair pathways and a large number of enzymes acting in each step do not allow a simple approach to their solutions. An MD simulation of lesion recognition may provide the stepwise description of biomolecular reactions at the radiation damage site through the capability to govern chemical and chemico-physical reactions in time intervals that correspond to real time of formation and breakage of chemical bonds (order of femtoseconds). The specific structural conformation and energetic properties of the lesion, determined by simulations, may be factors that guide a repair enzyme to discriminate a radiation lesion from an endogenous one as well as from native DNA part.

3. Method

The MD technique was the main tool used in simulations. Since a DNA molecule is not rigid, static structure, the x-ray diffraction and NMR results usually show average structural parameters. In reality, every DNA molecule is under constant thermal fluctuations, which result in local twisting, stretching, bending and unwinding of the double helix. MD is a simulation technique that yields static and dynamic properties of

a molecular system and thus may provide useful scientific data showing the DNA in its dynamical mode. The classical MD is based on solving Newton's equations of motion for each atom in the system. This way it is capable to simulate the behavior of a system consisting of N atoms. Solving these equations produces new atomic coordinates that can be used to calculate a new set of forces. Static and dynamic properties of the system are then obtained as time averages over the trajectory. For the simulations the MD program package AMBER 5.0 was used [15]. The potential energy function in AMBER 5.0 is calculated as contributions from bonds, single angles, torsional, and electrostatic functions as shown in Eq. 1.

$$E_{pot} = 1/2 \sum_{bonds} K_r (r - r_{eq})^2 + 1/2 \sum_{angles} K_\theta (\theta - \theta_{eq})^2 + 1/2 \sum_{dihedrals} K_\varphi [1 + \cos(n\varphi - \chi)] + \sum_{j=1}^{atoms} \sum_{i>j}^{atoms} \left[\left(\frac{R_{ij}^*}{r_{ij}} \right)^{12} - \left(\frac{R_{ij}^*}{r_{ij}} \right)^{6} + \frac{q_i q_j}{\varepsilon r_{ij}} \right] \quad \text{Eq. (1)}$$

where r, θ and φ are bond lengths, planar angles and dihedral angles, respectively; r_{eq} and θ_{eq} are their equilibrium values; r_{ij} is the distance between atoms i and j; q_i is the partial charge on atom i; ε is dielectric constant; K_r, K_θ, K_ϕ and R_{ij} are empirical parameters depending on atom types. The point charges q_i and q_j in a calculation of electrostatic function are centered on each atom and are derived by fitting to quantum mechanical electrostatic potential.

3.1 *Molecular dynamics protocol*

In a MD simulation, the simulated molecules were subjected to several hundred picosecond (ps) up to 1-2 nanosecond (ns) of MD simulation under molecular dynamics protocol consisting of the following sequential steps:

1. Preparation of solute molecule(s). Solute molecules were non-damaged DNA segments having certain part replaced by lesion (e.g. 8-oxoguanine). The structural and chemical parameters of the lesion were defined prior to insertion of modified part into the solute molecule. These parameters as lengths of chemical bonds, angles and charges were taken from existing experimental data where available, or for small molecules (up to several 10's atoms) were calculated by quantum chemical methods. The structures of modified solute molecules were then optimized using the program AMBER 5.0 in order to achieve stabile molecular configuration with minimal potential energy.
2. Locating the solute molecule into the simulation cell.
3. Neutralization of the negative charges of DNA phosphates by adding the sodium

counterions at the initial positions bisecting the O-P-O angle at a given distance (~5 Å) from each phosphorus atom.

4. Solvation of the solute molecules in the water (several 10 thousand's water molecules depending on the size of solute molecule were used).
5. Minimization of the potential energy of the system.
6. Heating up to a required temperature (e.g. 310K (36.85°C), close to human body temperature) during sequential MD runs.
7. Density stabilization of the system during constant pressure MD runs.
8. Production molecular dynamics with constant volume.

3.2 *Computational details*

Solvation of solute molecule requires a large number of water molecules that increase requirements on the capacity of RAM (Random Access Memory) and CPU (Central Processing Unit) time. To be able to handle such large systems, the original AMBER 5.0 code was partly parallelized and then installed on Fujitsu VPP5000 vector/parallel supercomputer using an auto-vectorizing compiler. Its sequential and parallel flags were changed in order to compile the program on the VPP5000 computer. After introducing these changes and required resizing, the program was able to deal with a system consisting of up to 100,000 atoms within reasonable CPU time. Production MD simulations were performed on the Fujitsu VPP5000 supercomputer or on the Hitachi SR8000 parallel supercomputer. Preparatory steps as formation of solute molecules, minimization, heating and density stabilization were performed on the scalar workstations (SUN). Supercomputers that were used in simulations are at the Center for Promotion of Computational Science and Engineering of the Japan Atomic Energy Research Institute. The samples of CPU simulation time required to accomplish 1 ps of MD are shown in Table 1.

3.3 *Analysis of electrostatic energy*

Electrostatic interactions are found to be the dominant factor in determining conformation of biomolecules, are significant in ligand-receptor binding and play an important role in the stability and function of biomolecules [16, 17].

Several electrostatic properties were calculated using the DelPhi program in order to evaluate the impact of DNA lesions on the DNA structure and the interaction of the lesions with surrounding environment. DelPhi is the program, which uses the finite difference method to solve the Poisson-Boltzmann (P-B) equation for molecules of arbitrary shape and charge distribution [18]. The P-B equation is solved for the system containing DNA molecule and Na^+ ions. The overall charge density in the system is obtained from the charges of the DNA adding the contributions from dissolved Na^+

ions:

$$\Delta\varepsilon(r)\Delta\varphi(r) = \rho_{macro}(r)\varphi + \sum_i q_i \eta_i^0 \exp^{-q_i\varphi(r)/kT} \qquad \text{Eq. 2}$$

where $\rho_{macro}(r)$ is the charge density due to the DNA and the sum of exponentials is the charge density due to the dissolved ions. (φ is the electrostatic potential in the region of space; ε is dielectric constant; q_i is the charge on Na^+; η_i^0 is the number density of ion i in the bulk solution; k is the Boltzman constant and T is the temperature). The electrostatic energy and van der Waals interactions are the only long-range non-bonded interactions in the potential energy function, (Eq. 1). Value of electrostatic energy is calculated for pairs of atoms that are separated by three or more bonds. Thus, it is assumed that the well-separated atoms were interacting mainly electrostatically since no cut-off distance was used in the calculation of the electrostatic interactions.

Electrostatic energy in AMBER 5.0 (4^{th} term of Eq. 1) is calculated as the sum over all atoms of the DNA molecule (or its part). This calculation is based on atom centered point charges and the sum runs over all atoms of the molecule. The electrostatic potential $\varphi(r)$ at a position r derived from Eq. 2 includes the contributions from all atoms of the molecule as well as from the Na^+ counterions in the environment. In this way, calculated electrostatic interaction includes factors originated by the entire molecular composition as well as from environment.

In performed MD simulations the constant dielectric function was used and 1-4 electrostatic interactions (electrostatic interactions separated by only three bonds) were scaled by factor 1.2, which is the recommended value for AMBER 5.0 force field. Particle Mesh Ewald Sum technique was used as implemented in AMBER 5.0 [19]. In this method a Gaussian charge distribution of opposite sign was superimposed upon the original point charges, producing a screened charge distribution. The electrostatic interactions between the screened charges were then short ranged. The original distribution was recovered by adding a second Gaussian charge distribution identical to the first, but of opposite sign. In the calculation of electrostatic interactions no cut-off distance was applied and thus all water molecules in system were included. The van der Waals interactions were calculated within the defined cut-off distance (10-12 Å). Periodic boundary conditions were applied throughout the entire simulation to eliminate undesirable edge effects.

4. Results and Discussion

4.1 *Thymine dimer*

Thymine dimmer (TD) is photolesion produced by UV radiation in sunlight and is one major factor causing the skin cancer. It is formed as a covalently bonded complex of

two adjacent thymines on the single strand of DNA. This damage is very frequent but almost 90% of TDs are repaired within short time of the order of minutes, and only few are experimentally observable and initiate future changes on cell level, [20].

This study was conducted with DNA dodecamer d(TCGCGT^TGCGCT)$_2$, where T^T indicates the thymine dimer, (Figure 1). The results of a 600 ps MD simulation shows that this lesion doesn't disrupt double helical structure and hydrogen bonds between complementary bases are well preserved throughout the simulation. Thymine dimer lesioned DNA, if compared with native one, has sharp bending at the TD site which is originated by the two covalent bonds C(5)-C(5) and C(6)-C(6) between the adjacent thymine bases forming the thymine dimer [21]. This bending discriminates lesion from the native DNA segment and produces conformation that facilitates formation of DNA-enzyme complex by complementary shapes of repair enzyme and bent DNA.

4.1.1 Complex of repair enzyme T4 Endonuclease V and TD lesioned DNA

Thymine dimer is repaired by the repair enzyme T4 Endonuclease V that slides on non-target sequences and progressively incises strand at all dimers within the DNA molecule. This enzyme binds to DNA double strand in two-step process: at first it scans non-target DNA by electrostatic interactions to search for damaged sites, and at second it sequentially specifically recognizes the dimer sites [22]. The entire process of binding T4 Endonuclease V to thymine dimer lesioned DNA was simulated with an existing MD method. Considering the limitations arising from the simulations of large systems and requirements for CPU time, the catalytic center of enzyme was only subjected to the simulations. Catalytic center of the enzyme is its active site: enzyme catalyzes reactions involving the joining of two reactants by providing active sites in which the substrates are bound closely together and properly oriented. Enzyme participates in the reaction with its substrate (e.g. DNA) by forming brief covalent bonds with the substrate, catalyzing reactions and then leaving the substrate.

The key amino acid of the enzyme T4 Endonuclease V are – glutamic acid 23 of which carboxyl chain plays a crucial role in the cleavage of N-glycosyl bond in DNA (base excision repair) together with surrounding nine amino acids (eight of H1 and two of H2 helices) were selected to form the simulated part of enzyme. Selection of amino acids was based on the crystal structure of DNA complexed with T4 Endonuclease V [23]. T4 Endonuclease V consists of three α helices (H1 - amino acids 14 through 38, H2 - 64 through 82 and H3 - 108 through 124) standing side-by-side, several reverse turns and several loops [24]. Glu-23, of which carboxyl chain plays a crucial role in the cleavage of N-glycosyl bond in DNA during an enzymatic repair pathway, is surrounded

by amino acids Arg-3, Arg-22 and Arg-26 belonging to helix H1. A side chain of Glu-23 also forms a hydrogen bond with the backbone amino group of Arg-3. Arg-3 and Thr-2 - two polar amino acids at the NH_2 terminus - form several hydrogen bonds with the side chains of helices H1 and H2, and lie on the molecular surface. Considering these properties, eight amino acids of H1 - Glu-20, Tyr-21, Arg-22, Glu-23, Leu-24, Pro-25, Arg-26, Val-27, and two amino acids at NH_2 terminus - Thr-2 and Arg-3 were selected to form the simulated part of the enzyme. The amino acids - Thr-2, Arg-22, Glu-23 and Arg-26, form so called catalytic center that is active in the incision of thymine dimer during a repair pathway, and together with other six selected amino acids - Arg-3, Glu-20, Tyr-21, Leu-24, Pro-25 and Val-27, lie at the central part of concave site of the enzyme. This part of enzyme may be easily exposed to the DNA surface and has extensive contacts with DNA in the crystal complex, (Figure 2).

After nearly 100 ps of the MD simulation, the catalytic part of enzyme approached the DNA at the thymine dimer site, docked onto it, and this complex remained stable afterwards (the simulation was performed for 500 ps), (Figure 3). When the same simulation was performed with the non-lesioned native DNA molecule, the catalytic center didn't fuse into the DNA molecule and the DNA-enzyme complex was not formed [25].

The above conclusions derived from the simulation of DNA-enzyme complex shall be limited to the description of situation at the docking of catalytic center into DNA. The entire recognition process would require a simulation of the whole enzyme molecule that would include the role of secondary structure of the enzyme in the formation of the complex. This sort of simulation was not performed due to the limitations of available computational environment.

4.1.2 Electrostatic energy analysis

In consideration of factors that contributed to the formation of the complex of TD lesioned DNA and catalytic center, the electrostatic interaction energy between the dimer lesion and catalytic center was calculated. It has been found that while the electrostatic energy of thymine dimer is negative around –9 kcal/mol (Table 2, Figure 4), the electrostatic energy of glutamic acid 23 (the closest amino acid to the C5' atom of phosphodiester bond of dimer) is around +10 kcal/mol (Figure 5). Glutamic acid 23 is key amino acid at the repair pathway located close to the C5' end of phosphodiester bond of TD. After the enzyme approached the DNA surface, the energy became negative, which was mainly originated by two arginines (Arg-22 and Arg-26) which both are having highly negative electrostatic energy of around -50 kcal/mol [21], and were located at the close positions to DNA. This, in combination with negative charge

of DNA phosphate backbone, creates repulsive environment, in which the enzyme is already docked into the DNA.

The calculated values of electrostatic energy that represent the total electrostatic interactions in the selected molecules were calculated by using the Particle Mesh Ewald Sum technique for infinite simulated volume of repeating units through periodic boundary conditions; i.e. no cut-off distance was applied. Since the electrostatic energy of the native thymine is nearly 0 kcal/mol (Table 2), the specific value of electrostatic energy at the TD site represents a factor discriminating the thymine dimer lesion from the native thymine [21].

4.2 *Thymine glycol*

Thymine glycol (TG) is lesion observed in DNA after irradiation *in vitro* as well as *in vivo*, and after oxidation by chemicals (Figure 6). Thymine glycol is known as causing Cockayne Syndrome - an inherited disorder in which people are sensitive to sunlight, have short stature and appearance of premature aging. This lesion is repaired with the repair enzyme Endonuclease III, which removes a number of damaged pyrimidines from DNA via its glycosylase activity, and cleaves the phosphodiester backbone at apurinic/apyrimidinic sites via an ß-elimination mechanism. To study the time evolution of the recognition processes of TG lesioned DNA by the repair enzyme Endonuclease III, the MD simulations of the following molecules were performed [26, 27]:

- DNA 30-mer d(CCAGCGCACGACGCA'TG'GCACGACGACCGGG)$_2$ where 'TG' refers to thymine glycol;
- repair enzyme Endonuclease III.

The analysis of the results of 1 ns MD simulation shows that the double helical structure and hydrogen bonding are well kept through the simulation (except the base pair of cytosine C5' – guanine C3' end, in which hydrogen bond pairing collapsed after 850 ps). DNA began to bend at the thymine glycol site after 500 ps of the simulation and the bending continued until the simulation was terminated. At the TG site the kink was observed, that relocated TG closer to DNA surface. Bending associated with the kink at TG site dislocated glycosyl bond at C5' atom closer to DNA surface, enabling it to be approached by the repair enzyme, (Figure 7).

As far as the movement of repair enzyme Endonuclease III is concerned, the enzyme was constantly moving toward the surface of DNA in two directions. One direction was toward the surface of DNA and second one was closer toward the center of DNA. From the original position (closest atoms at distance around 6 Å,), it moved as close as around 2 Å at 300 ps. Distance of 2 Å is close enough to form the Van der

Waals contact between surface atoms. In addition to this movement, the enzyme also rotated around x-axis. This rotation caused that the surface area surrounding glutamic acid was facing to DNA surface. Glutamic acid is the amino acid of enzyme that was found localized close to C3' atom of TG upon formation of complex [27].

4.2.1 Electrostatic energy analysis

Intermolecular electrostatic interactions were calculated between enzyme and DNA 30-mer throughout the simulation. In the beginning of MD simulation, energy had a positive value (~ +10 kcal/mol). After molecules approached each other (distance around 2 nm), the electrostatic interaction became negative (~ –20 kcal/mol). Upon formation of the complex with repair enzyme Endonuclease III, the electrostatic interaction changed to the value of around –40 kcal/mol (distance of closest atoms ~1.6 Å), [26].

The electrostatic energy of nucleotide with TG is negative at value of –26 kcal/mol (Table 2). This negative electrostatic energy is probably one factor contributing to proper recognition of TG lesion by the enzyme, and discriminates TG from native thymine (~ 0 kcal/mol), [21].

4.3 *8-oxoguanine*

8-oxoguanine (8-oxoG) is formed by an oxidation of a guanine base in DNA, (Figure 8). It is considered to be one of the major endogenous mutagens contributing broadly to spontaneous cell transformation. Its frequent mis-pairing with adenine during replication increases the number of G-C → T-A transversion mutations. This mutation is the most common somatic mutation in human cancers. The 8-oxoguanine is recognized and subsequently repaired by the DNA glycosylase (hOGG1 in humans). DNA glycosylases acting on single-base lesions use an extrahelical repair mechanism during which the enzyme recognizes oxidative damaged guanines and excludes normal DNA bases. The study on the 8-oxoguanine lesion was aimed to describe structural and energetic changes on the DNA molecule that are caused by this lesion, and to discuss how these changes may be significant in formation of a complex with the repair enzyme. The MD simulation (2 ns) was performed for two B-DNA molecules:

- (native DNA 15-mer, $d(GCGTCCAGGTCTACC)_2$;
- 8-oxoG lesioned DNA 15-mer, $d(GCGTCCA'8\text{-}oxoG'GTCTACC)_2$, where 8-oxoG refers to 8-oxoguanine.

In the 8-oxoguanine lesioned DNA molecule the disruptions of weak hydrogen bonds between respective bases caused locally collapsed B-DNA structure. While the hydrogen bonds between 8-oxoguanine and opposite cytosine 23 were well kept, the neighboring base pairs (adenine 7 – thymine 24, and guanine 9 – cytosine 22) were

broken. The hydrogen bonding of base pair thymine 10 – adenine 21 ceased to exist very early (after around 50 ps of MD simulation). In the case of the native DNA the B-DNA structure around native guanine 8 was well preserved.

Adenine 21 on the complementary strand (separated from 8-oxoguanine by one base pair) was completely flipped-out of DNA double helix (Figure 9). This extrahelical position was caused by the disrupted hydrogen bonds and by the strong electrostatic repulsion between the atoms in the region. The cytosine 22 was also severely dislocated form its intrahelical position and its hydrogen bonding to guanine 9 was not existing. The extrahelical position of adenine 21 formed a hole in the double helix that might favor docking of repair enzyme into DNA during a repair pathway. The flipped-out base might also be inserted into the enzyme cavity further ensuring the stability of DNA-enzyme complex [28].

4.3.1 Electrostatic energy analysis

The electrostatic energy of the 8-oxoG is –48 kcal/mol that discriminates this lesion form the native guanine (~ –37 kcal/mol), (Table 2). To evaluate the impact of the 8-oxoG lesion on the DNA molecule the intermolecular electrostatic interactions were calculated between the nucleotide with 8-oxoG and the neighboring nucleotides with respective bases (cytosine 6, adenine 7, guanine 9, thymine 10, adenine 21, cytosine 22, cytosine 23, thymine 24 and guanine 25). Interaction energy was calculated between two groups of atoms: atoms belonging to the nucleotide with 8-oxoG as one group, and atoms of the respective neighboring nucleotide as second group. During the 1 ns of MD simulation the electrostatic interaction energy in lesioned DNA largely oscillated around an average value of around 21 kcal/mol (Figure 10). The positive value of the interaction electrostatic energy between the lesion and the rest of DNA represents repulsion that may cause the disruption of hydrogen bonds in the vicinity of the lesion and also may contribute to the lesser stability of the surrounding atoms. This electrostatic repulsion between the atoms in the region and disruption of hydrogen bonds caused extrahelical position of adenine 21 as discussed above. The electrostatic interaction energy calculated for the nucleotide with the native guanine 8 in the non-lesioned DNA is less repulsive and has a stable average value of 7.5 ± 1.4 kcal/mol.

5. Conclusions

The present paper comprises of the results of MD simulation of several radiation and oxidative lesions on DNA molecules. There were studied two pyrimidine base lesions –thymine dimer and thymine glycol, and one purine lesion – 8-oxoguanine. Except thymine glycol the other two lesions are considered to originate neoplasic

transformation of the cell and are found in human cancers. The summary of structural and energy specific properties initiated by each lesion are shown in Table 2. The common features observed for all lesions are the specific conformation originated at the lesions site, like disruption of hydrogen bonding networks (8-oxoguanine), sharp bending at the lesion site (thymine dimer, thymine glycol), flipping-out the base on the strand complementary to the lesion and specific values of the electrostatic interaction energy at the lesion (8-oxoguanine). Among these changes the most important is considered the flipping-out base since it creates the empty space in the DNA double strand and this space may serve as a template for the docking of the enzyme and for the formation of the DNA-enzyme complex. The strong bending that was observed in the thymine dimer lesioned DNA molecule forms a complementary shape in respect to the repair enzyme T4 Endonuclease V and facilitate the formation of complex. The electrostatic interaction energy at several lesion sites differs from its values at the native DNA site (thymine dimer, thymine glycol, 8-oxoguanine) and is considered as contributing to the proper recognition of the respective lesion by discriminating the lesion from the native site. This recognition is important during electrostatic scanning of the DNA surface by the repair enzyme. The results on 8-oxoguanine lesioned DNA were performed for naked DNA only and did not include the repair enzyme. In this aspect they may serve as a template for theoretical study of the specific recognition mechanism of the DNA human repair enzyme 8-oxoguanine DNA glycosylase (hOGG1) with its substrate – the DNA containing 8-oxoG.

The results of MD simulation, in addition to the existing crystallographic and molecular biology techniques, may contribute to the studies of radiation risk and DNA radiation damage repair by the dynamical description of the structural and chemical processes that are undergoing at the lesioned DNA molecule. It may also contribute to the determination of the key factors in the process of recognition of the lesion by the repair enzyme. The detail knowledge of these processes would help to quantify and qualify the chemical processes that lie behind the cellular and tissue changes originated by radiation and this way indirectly determine the involved radiation risk.

Acknowledgments

The author acknowledges Mr. Toshiyuki Nemoto of The Research Organization for Information Science and Technology for the installation, maintenance and adjustment of the AMBER 5.0 code on supercomputers VPP5000 and SR8000. The valuable support from the all members of The Radiation Risk Analysis Laboratory, JAERI Tokai Research Establishment is also highly acknowledged.

References

1. Hanawalt, P.C. Mutat Res. 400 (1-2), (1998), 117.
2. Bartram, C.R. Eur. J. Pediatr., 135 (2), (1980), 121.
3. Jaspers, N.G. Cytokines Mol. Ther., 2 (2), (1996), 115.
4. http://saturn.roswellpark.org/cmb/huberman/DNA_Repair/damage_types.html
5. in Cancer Medicine, 6th Edition, ed. Bast, R.C. et al, 2003, BC Decker Inc.
6. Harrison, S. and Aggarwal, A. Annu. Rev. Biochem. 59 (1990) 933.
7. Gicquel-Sanzey, B. and Cossart, P. EMBO J. 1 (1982) 591.
8. Ham, J., Thompson, A., Nedham, M., Webb, P. and Parker, M. Nucleic Acid Res. 16:12 (1988) 5263.
9. Beato, M. Cell 56 (1989) 335.
10. Harris, L, Sullivan, M. and Hickok, D. Computers and Mathematics with Applications 20 (1990) 25.
11. Marx, J. Science 229 (1985) 846.
12. Matthews, B. Nature 335 (1988) 294.
13. Harris, L, Sulliwan, M. and Hickok, D. Proc. Natl. Acad. Sci. USA 90 (1993) 5534.
14. Sources and Effects of Ionizing Radiation. UNSCEAR 2000 Report, UN, New York 2000.
15. Case, D.A., Pearlman, D.A., Caldwell, J.W., Cheathman III, T.E., Ross, W.S., Simmerling, C.L., Darden, T.A., Merz, K.M., Stanton, R.V., Cheng, A.L., Vincent, J.J., Crowley, M., Ferguson, D.M., Radmer, R.J., Seibel, G.L., Weiner, P.K. and Kollman, P.A., AMBER 5.0, (1997) University of California San Francisco.
16. Yang, A.S. and Honig B. Curr. Opin. Struct. Biol. 2 (1992) 40.
17. Gilson, M.K. and Honig B.H. Nature 330 (1987) 84.
18. Honig, B. and Nicholls, A. Science 268 (1995) 1144.
19. Smith, P.E. and Petit, B.M. J. Chem. Phys. 105 (1996) 4289.
20. Brash, D.E., Rudolph, J.A., Simon, J.A., McKenna, G.J., Baden, H.P., Halperin, A.J. and Pomten, J.A. Natl. Acad. Sci. USA 88, 1991, 10124.
21. Pinak, M. .J.Mol.Struct.:THEOCHEM 466 (1999) 219.
22. Dodson, M.L., Schrock, R.D. III and Lloyd, R.S. Biochemistry 32 (1993) 8264.
23. Vassylyev, D.G., Kashiwagi, T., Mikami, Y., Ariyoshi, M., Iwai, S., Ohtsuka, E. and Morikawa, K. Cell 83 (1995) 773.
24. Morikawa, K., Matsumoto, O., Tsujimoto, M., Katayanagi, K., Ariyoshi, M., Doi, T., Ikehara, M., Inaoka, T. and Ohtsuka, E. Science 256 (1992) 523.
25. Pinak, M. .J.Mol.Struct.:THEOCHEM 499 (2000) 57.
26. Pinak, M. JAERI-research 2001-038, (2001).

27. Pinak, M. J.Comput.Chem. Vol. 22, Iss.15 (2001) 1723.
28. Pinak, M. J.Mol.Struct.:THEOCHEM 583/1-3 (2002) 189.

Table 1 CPU simulation time required to accomplish 1 ps of MD simulation of the system composing of 40,000 atoms.

Machine / Execution type	SUN BLADE 1000, scalar	SR8000 scalar-parallel	VPP5000 vector-parallel
	Execution time		
CPU (750MHz), scalar	248 s		
1 CPU (VU-9.6Gflops, 333MHz), scalar			2434 s
1 CPU, vector			286 s
4 CPU, vector-parallel			91 s
1 CPU (1.56Gflops, 375 MHz), scalar		1914 s	
1 node (8 CPU), parallel		316 s	
4 node (32-CPU), parallel		179 s	

Table 2 Summary of structural and energy value changes in DNA initiated by the respective lesion. The electrostatic energy was calculated by the classical mechanistic approach using the point charges of atoms (4^{th} term of Eq.1).

native base	lesion	structural changes	electrostatic energy [kcal/mol]
guanine			-37
	8-oxoguanine	bending flipped-out base disruption of hydrogen bonds	-48
thymine			0
	thymine dimer	bending	-9
	thymine glycol	bending	-26

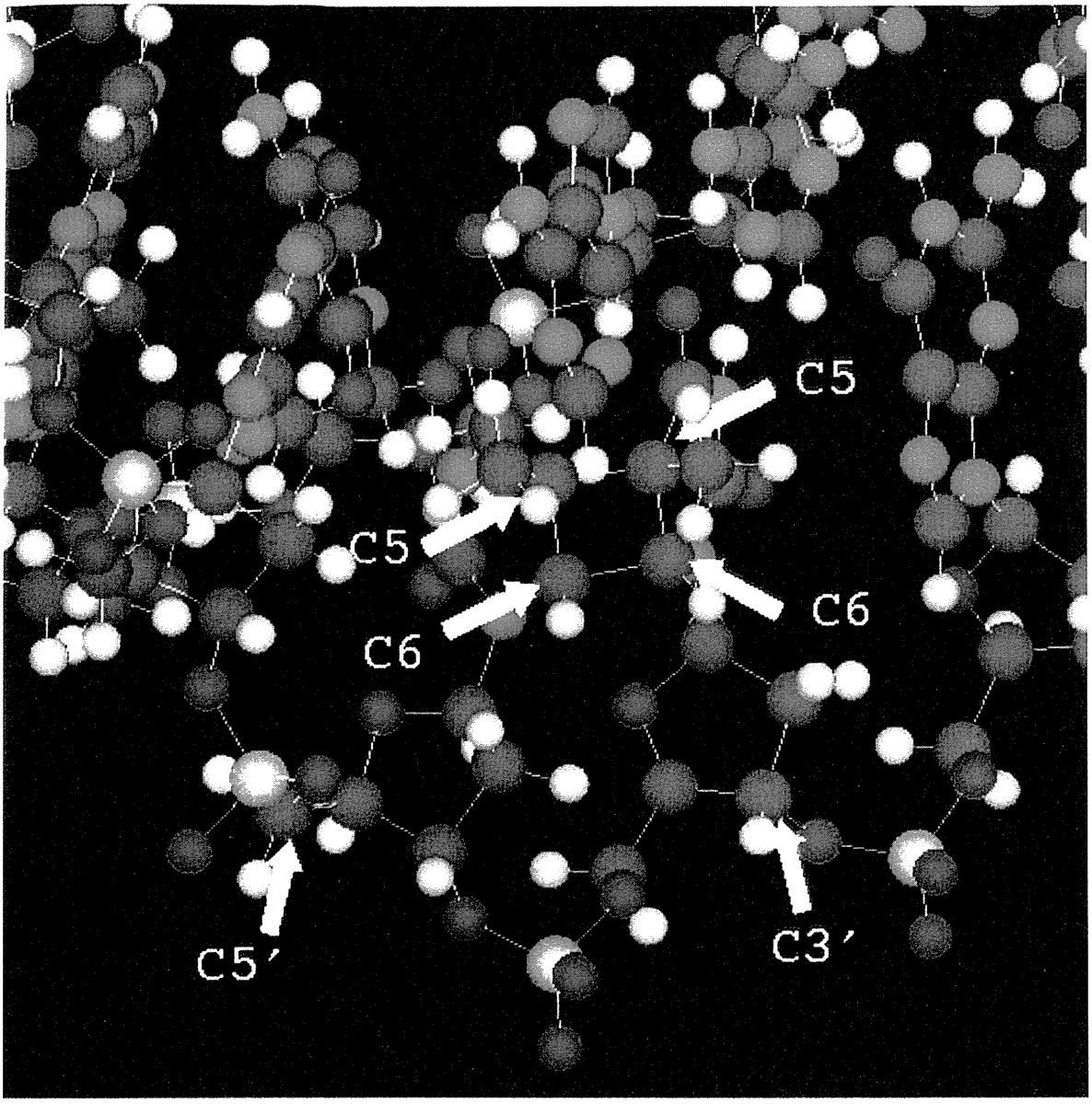

Figure 1 Thymine dimer inside the DNA dodecamer as a composition of two adjacent thymine bases covalently joined between C(5)-C(5) and C(6)-C(6) atoms of adjacent thymine bases.

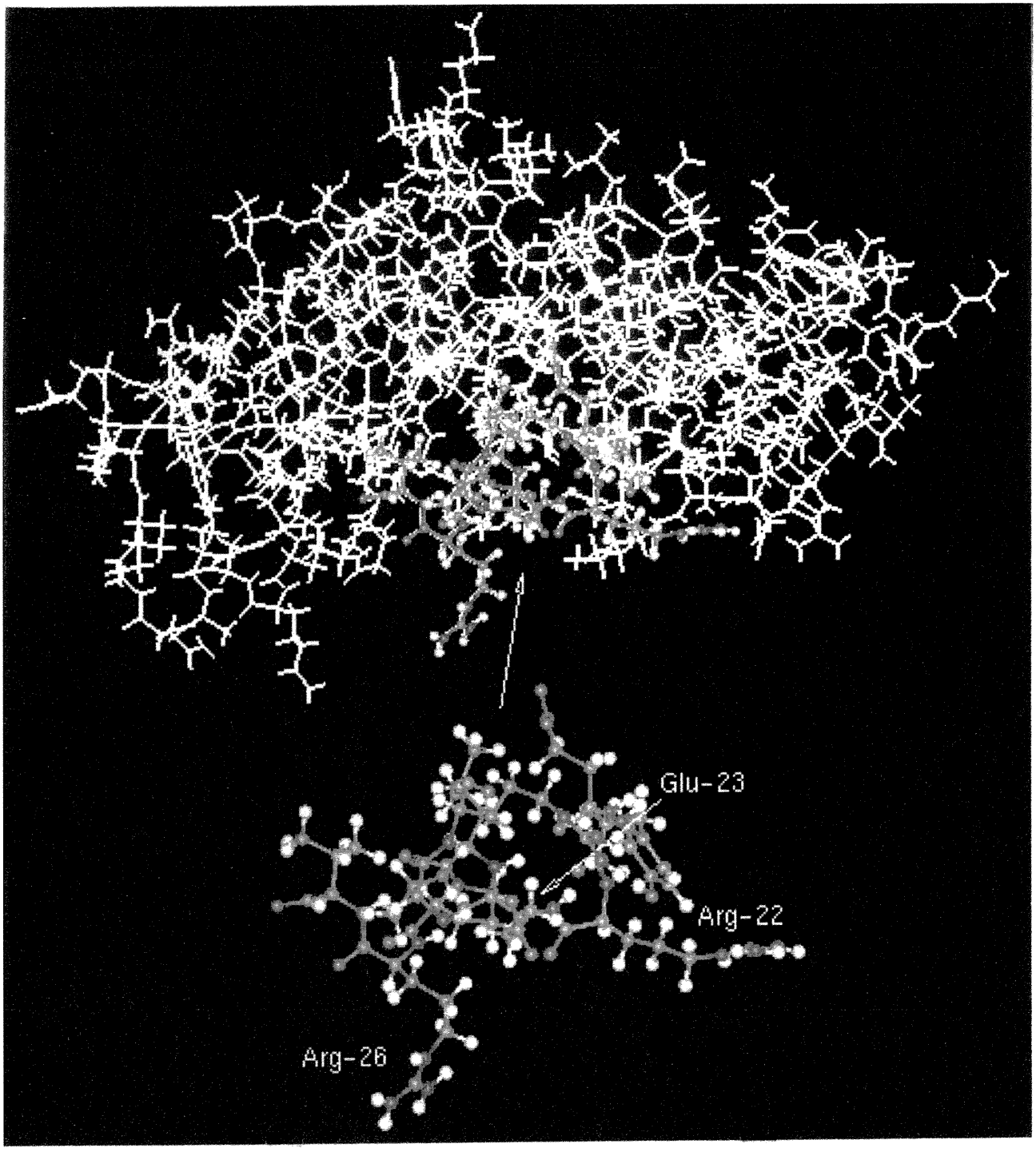

Figure 2 Catalytic center of T4 Endonuclease V, (amino acids - Thr-2, Arg-22, Glu-23 and Arg-26).

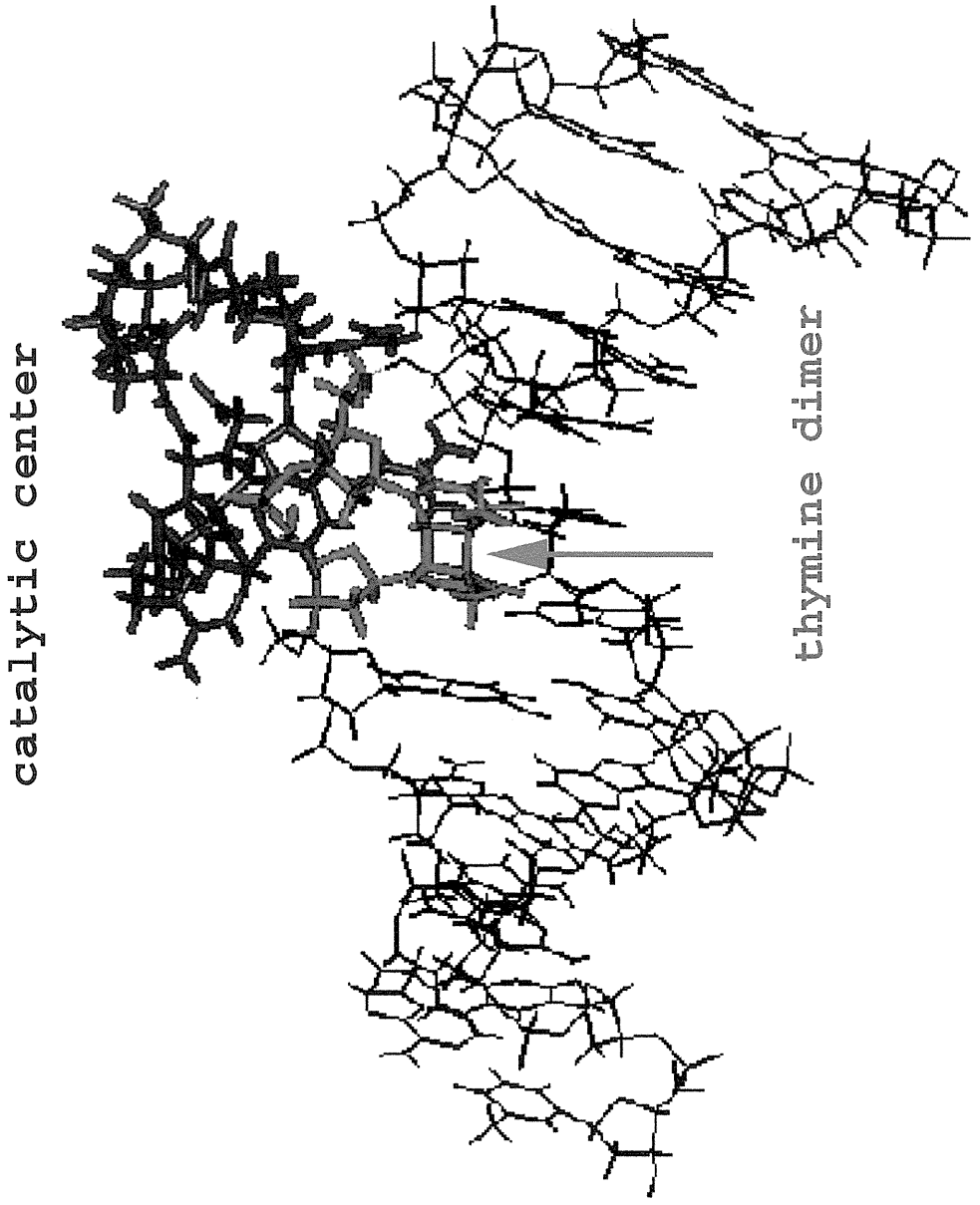

Figure 3 Complex of thymine dimer lesioned DNA molecule with catalytic center of repair enzyme T4 Endonuclease V formed during 100 ps of MD simulation. (green - thymine dimer, red - catalytic center)

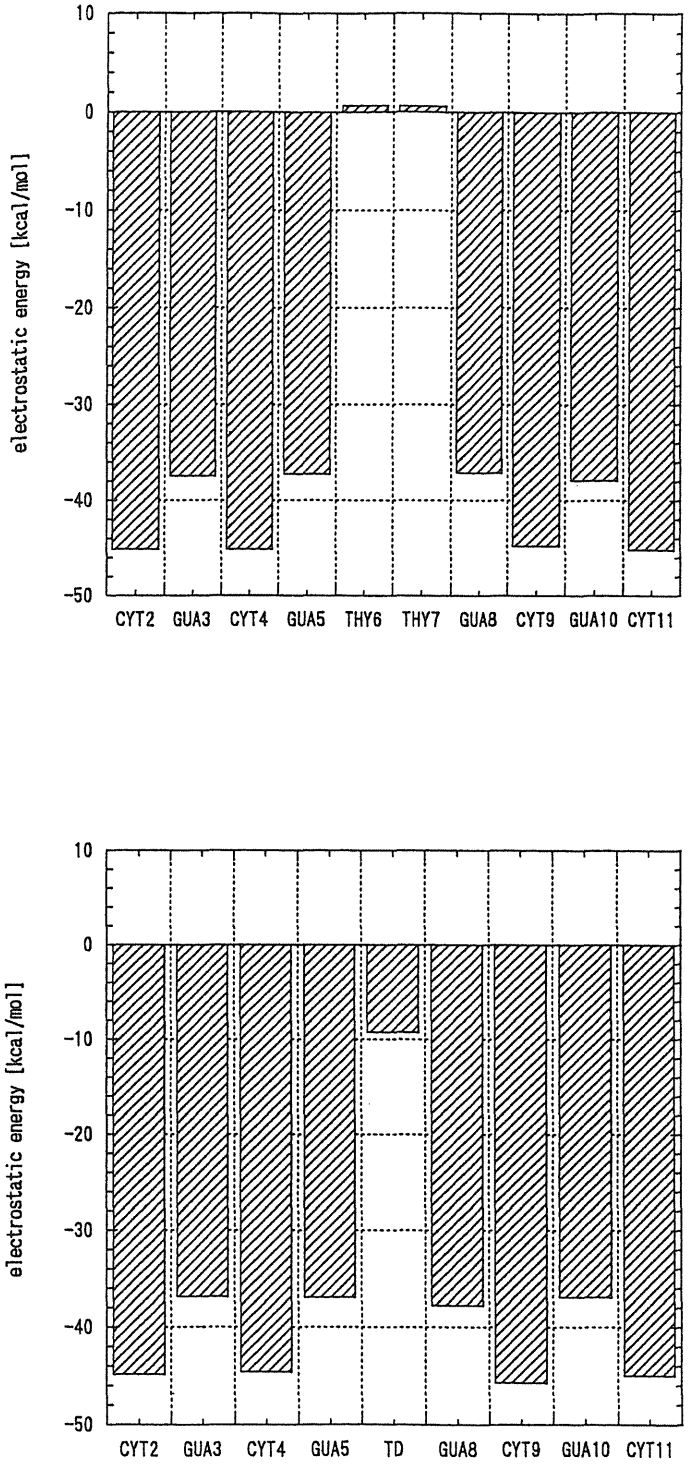

Figure 4 Electrostatic energy of DNA dodecamer bases a) native dodecamer b) dodecamer with TD.
The electrostatic energy of TD is negative around -9 kcal/mol and energy of native thymine is nearly 0 kcal/mol.

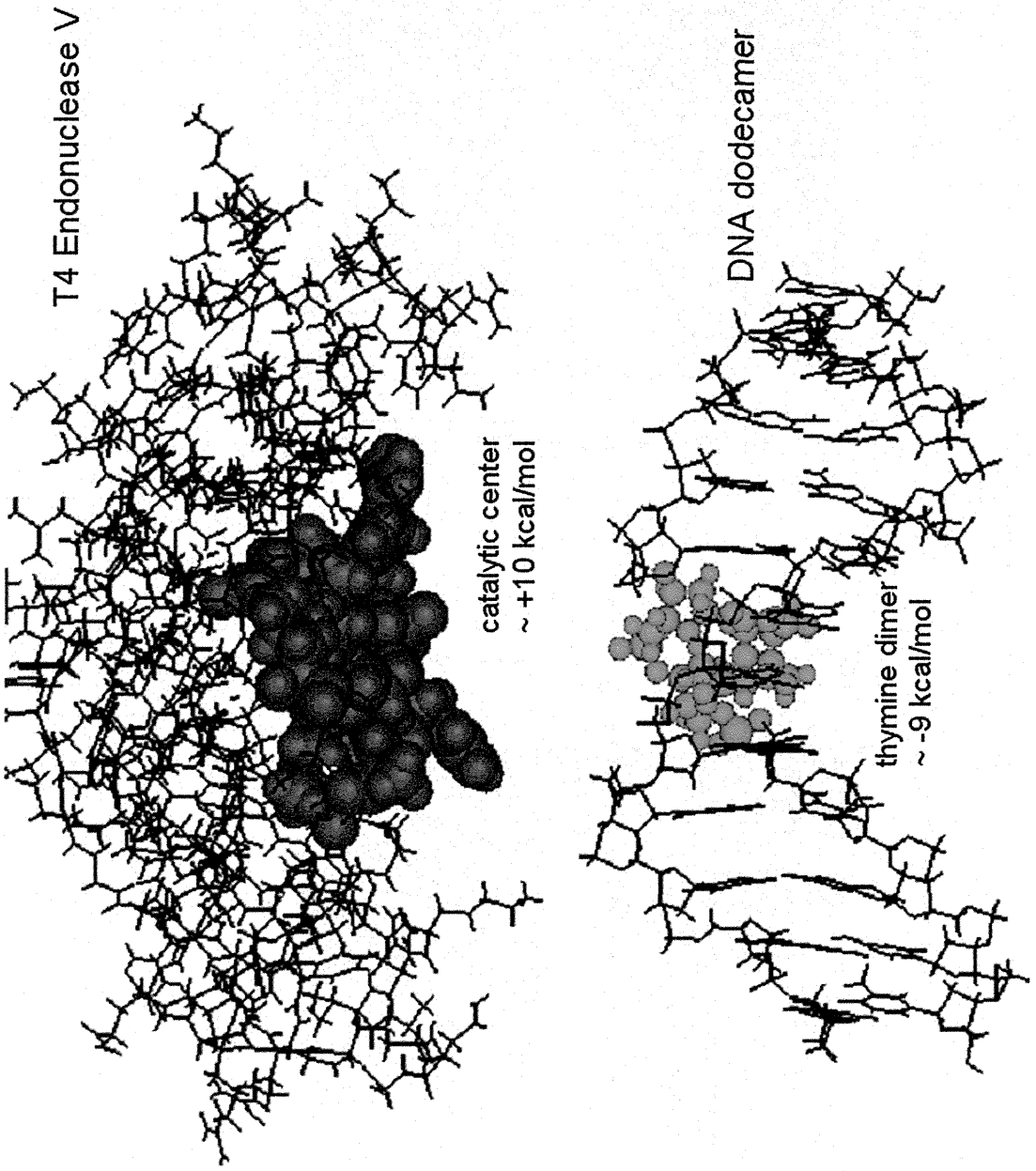

Figure 5 Complementary shape of repair enzyme T4 Endonuclease V and dodecamer with TD. The electrostatic energy of glutamic acid 23 is nearly 10 kcal/mol and the one of thymine dimer is negative around –9 kcal/mol. Glutamic acid 23 is key amino acid at the repair pathway located close to the C5' end of phosphodiester bond of TD.

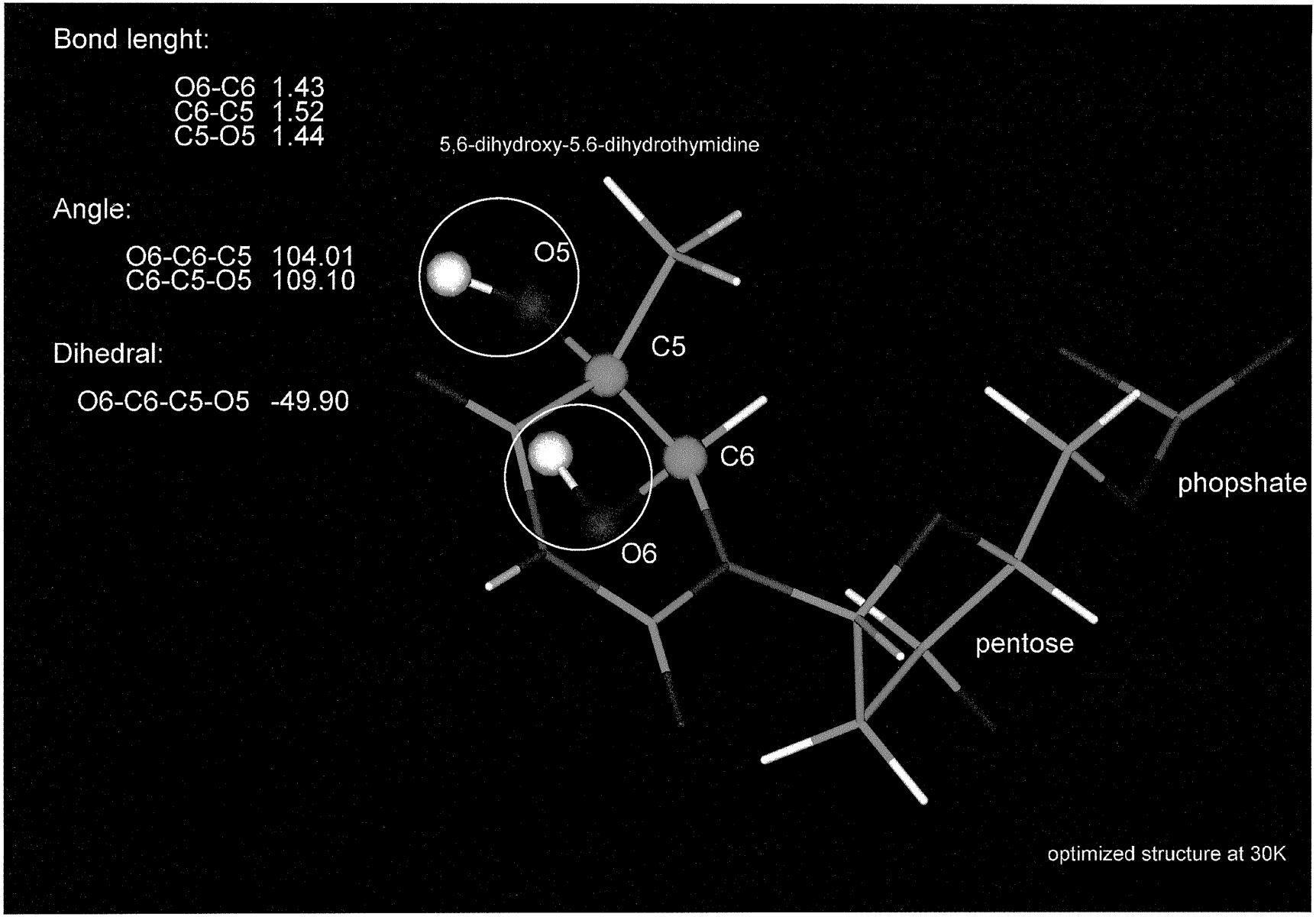

Figure 6 Molecule of the thymine glycol (5,6-dihydroxy-5,6-dihydrothymidine). Molecule was optimized at 30 K (bond lengths are in Å, angles in degrees). Encircled are hydroxyl groups oxidizing atoms C5 and C6.

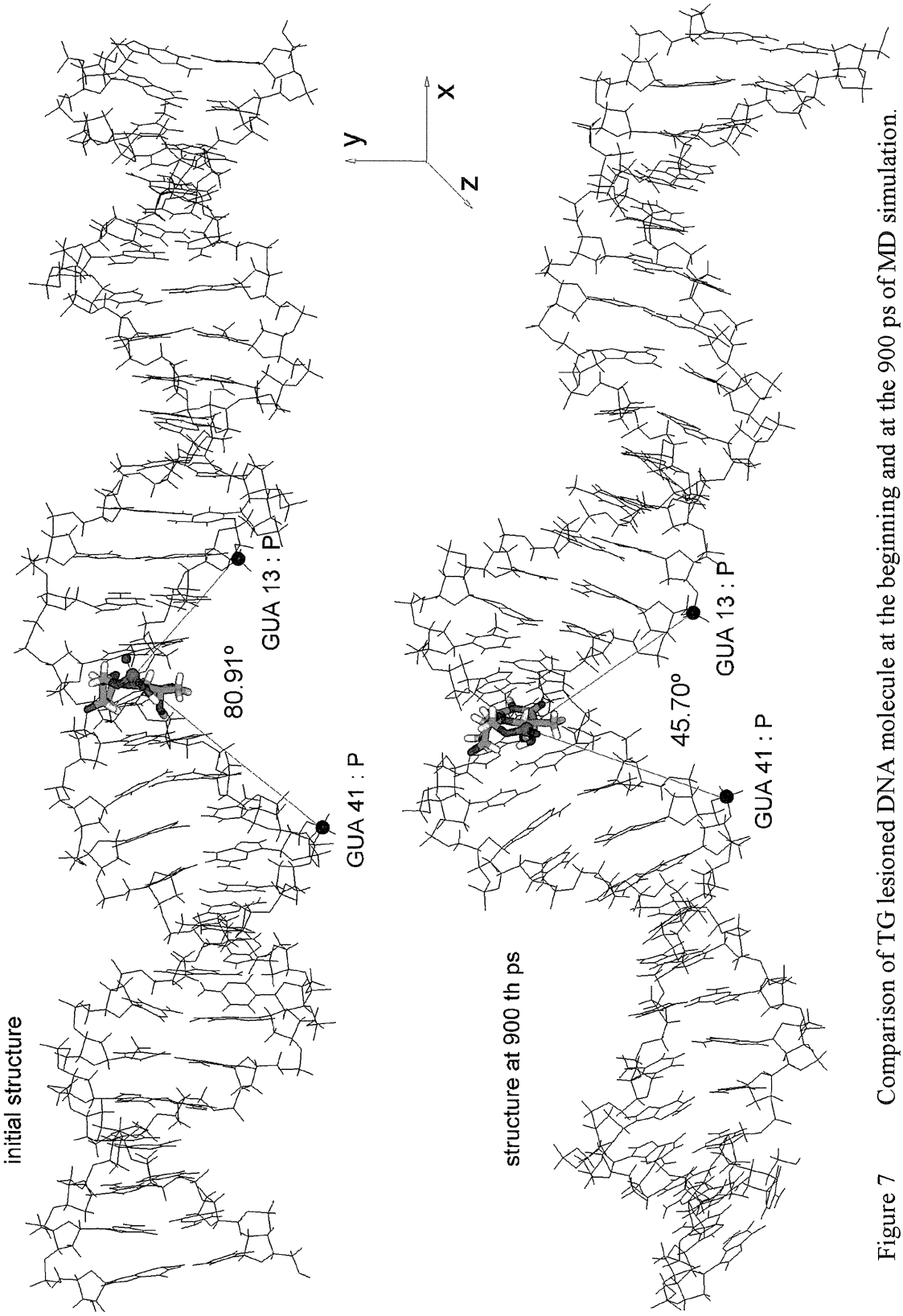

Figure 7 Comparison of TG lesioned DNA molecule at the beginning and at the 900 ps of MD simulation. The cytosine C5' end and guanine C3' end of DNA molecule are shown. It is seen that the molecule is bent and kinked at the thymine glycol site (colored atoms). Bending is expressed as the value of angle measured between phosphates of the guanine (position 41), thymine glycol (position 16, color atoms) and guanine (position 13).

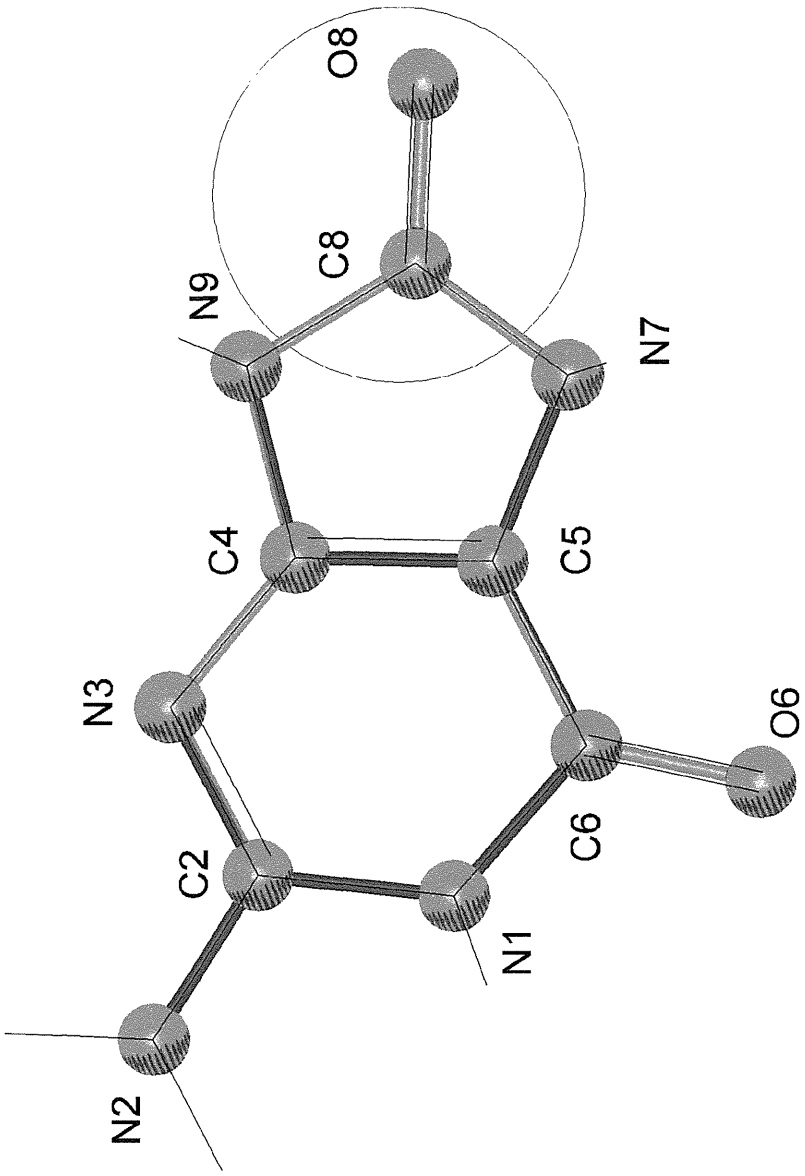

Figure 8 Molecule of 8-oxoguanine (7,8-dihydro-8-oxoguanine).

Encircled are the oxygen 8 (O8) and carbon 8 (C8).

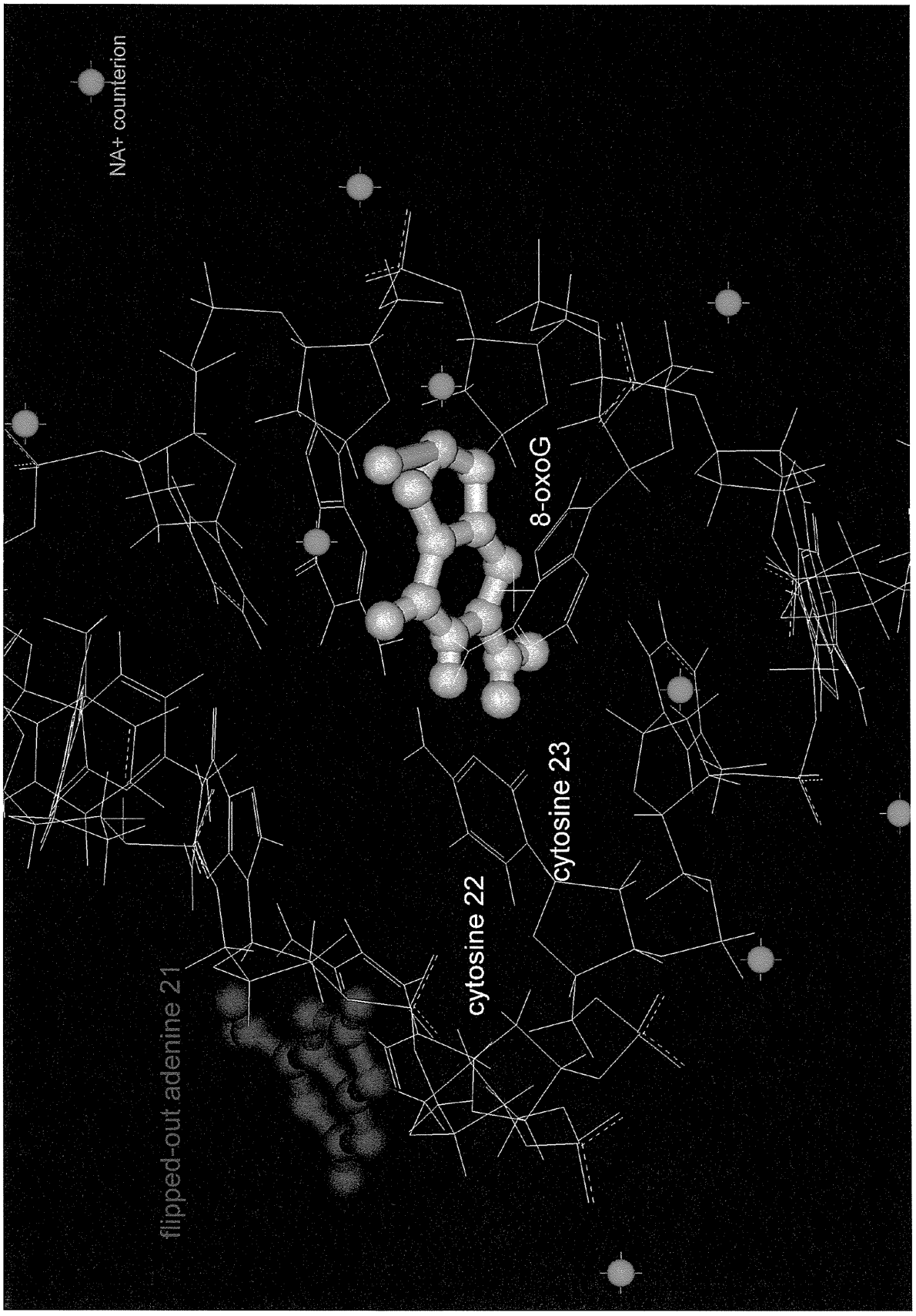

Figure 9 Flipped-out adenine 21 on the complementary strand to strand with 8-oxoG. The figure also indicates non-existence of hydrogen bonds between guanine 9 and cytosine 22, since the cytosine 22 is severely dislocated from its intrahelical position.

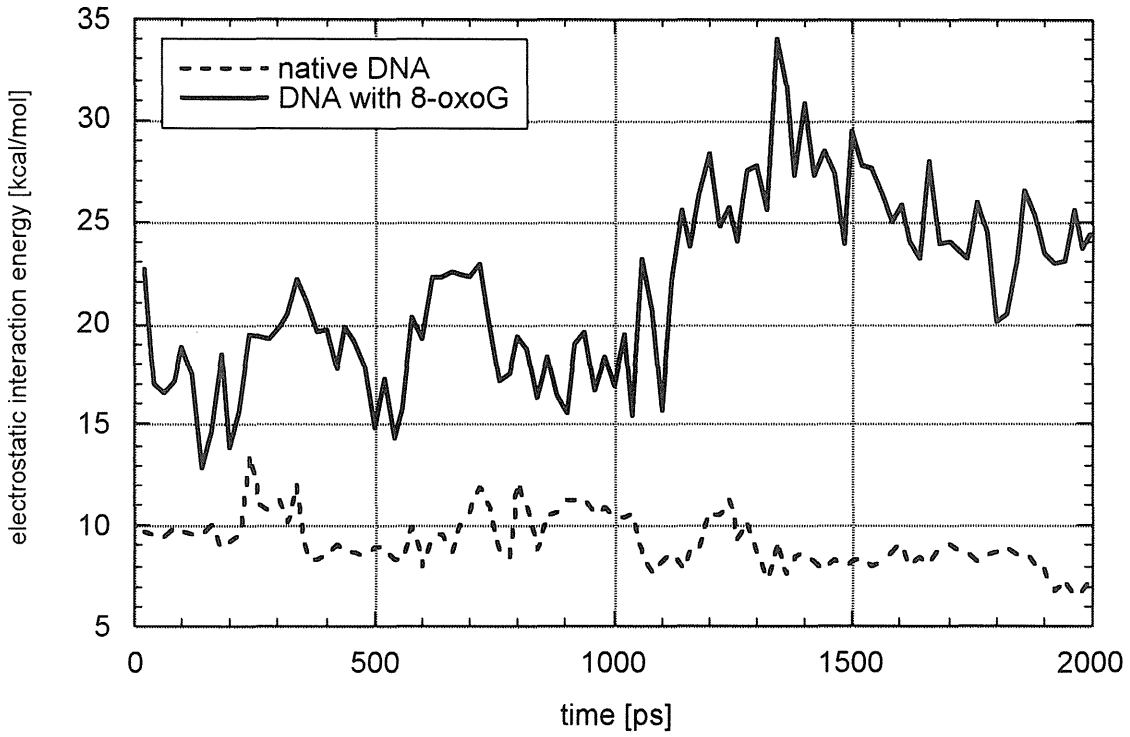

Figure 10 The intermolecular electrostatic interaction between the nucleotide with 8-oxoG and the neighboring nucleotides with respective bases (cytosine 6, adenine 7, guanine 9, thymine 10, adenine 21, cytosine 22, cytosine 23, thymine 24 and guanine 25). The electrostatic interaction energy in lesioned DNA largely oscillated around an average value of around 21 kcal/mol. The electrostatic interaction energy calculated for the nucleotide with the native guanine 8 has a stable average value of 7.5 ± 1.4 kcal/mol.

This is a blank page.

国際単位系（SI）と換算表

表1　SI基本単位および補助単位

量	名称	記号
長さ	メートル	m
質量	キログラム	kg
時間	秒	s
電流	アンペア	A
熱力学温度	ケルビン	K
物質量	モル	mol
光度	カンデラ	cd
平面角	ラジアン	rad
立体角	ステラジアン	sr

表2　SIと併用される単位

名称	記号
分，時，日	min, h, d
度，分，秒	°, ′, ″
リットル	l, L
トン	t
電子ボルト	eV
原子質量単位	u

1 eV=1.60218×10^{-19}J

1 u=1.66054×10^{-27}kg

表5　SI接頭語

倍数	接頭語	記号
10^{18}	エクサ	E
10^{15}	ペタ	P
10^{12}	テラ	T
10^{9}	ギガ	G
10^{6}	メガ	M
10^{3}	キロ	k
10^{2}	ヘクト	h
10^{1}	デカ	da
10^{-1}	デシ	d
10^{-2}	センチ	c
10^{-3}	ミリ	m
10^{-6}	マイクロ	μ
10^{-9}	ナノ	n
10^{-12}	ピコ	p
10^{-15}	フェムト	f
10^{-18}	アト	a

表3　固有の名称をもつSI組立単位

量	名称	記号	他のSI単位による表現
周波数	ヘルツ	Hz	s^{-1}
力	ニュートン	N	m·kg/s^2
圧力，応力	パスカル	Pa	N/m^2
エネルギー,仕事,熱量	ジュール	J	N·m
工率，放射束	ワット	W	J/s
電気量，電荷	クーロン	C	A·s
電位，電圧，起電力	ボルト	V	W/A
静電容量	ファラド	F	C/V
電気抵抗	オーム	Ω	V/A
コンダクタンス	ジーメンス	S	A/V
磁束	ウェーバ	Wb	V·s
磁束密度	テスラ	T	Wb/m^2
インダクタンス	ヘンリー	H	Wb/A
セルシウス温度	セルシウス度	℃	
光束	ルーメン	lm	cd·sr
照度	ルクス	lx	lm/m^2
放射能	ベクレル	Bq	s^{-1}
吸収線量	グレイ	Gy	J/kg
線量等量	シーベルト	Sv	J/kg

表4　SIと共に暫定的に維持される単位

名称	記号
オングストローム	Å
バーン	b
バール	bar
ガル	Gal
キュリー	Ci
レントゲン	R
ラド	rad
レム	rem

1 Å=0.1nm=10^{-10}m

1 b=100fm^2=10^{-28}m^2

1 bar=0.1MPa=10^5Pa

1 Gal=1cm/s^2=10^{-2}m/s^2

1 Ci=3.7×10^{10}Bq

1 R=2.58×10^{-4}C/kg

1 rad=1cGy=10^{-2}Gy

1 rem=1cSv=10^{-2}Sv

（注）

1．表1－5は「国際単位系」第5版，国際度量衡局 1985年刊行による。ただし,1 eVおよび1 uの値はCODATAの1986年推奨値によった。

2．表4には海里，ノット，アール，ヘクタールも含まれているが日常の単位なのでここでは省略した。

3．barは，JISでは流体の圧力を表わす場合に限り表2のカテゴリーに分類されている。

4．EC閣僚理事会指令ではbar，barnおよび「血圧の単位」mmHgを表2のカテゴリーに入れている。

換　算　表

力

N(=10^5dyn)	kgf	lbf
1	0.101972	0.224809
9.80665	1	2.20462
4.44822	0.453592	1

粘　度　1 Pa·s(N·s/m^2)=10 P(ポアズ)(g/(cm·s))

動粘度　1m^2/s=10^4St(ストークス)(cm^2/s)

圧力

MPa(=10bar)	kgf/cm^2	atm	mmHg(Torr)	lbf/in^2(psi)
1	10.1972	9.86923	7.50062×10^3	145.038
0.0980665	1	0.967841	735.559	14.2233
0.101325	1.03323	1	760	14.6959
1.33322×10^{-4}	1.35951×10^{-3}	1.31579×10^{-3}	1	1.93368×10^{-2}
6.89476×10^{-3}	7.03070×10^{-2}	6.80460×10^{-2}	51.7149	1

エネルギー・仕事・熱量

J(=10^7 erg)	kgf·m	kW·h	cal(計量法)	Btu	ft·lbf	eV
1	0.101972	2.77778×10^{-7}	0.238889	9.47813×10^{-4}	0.737562	6.24150×10^{18}
9.80665	1	2.72407×10^{-6}	2.34270	9.29487×10^{-3}	7.23301	6.12082×10^{19}
3.6×10^6	3.67098×10^5	1	8.59999×10^5	3412.13	2.65522×10^6	2.24694×10^{25}
4.18605	0.426858	1.16279×10^{-6}	1	3.96759×10^{-3}	3.08747	2.61272×10^{19}
1055.06	107.586	2.93072×10^{-4}	252.042	1	778.172	6.58515×10^{21}
1.35582	0.138255	3.76616×10^{-7}	0.323890	1.28506×10^{-3}	1	8.46233×10^{18}
1.60218×10^{-19}	1.63377×10^{-20}	4.45050×10^{-26}	3.82743×10^{-20}	1.51857×10^{-22}	1.18171×10^{-19}	1

1 cal= 4.18605J（計量法）

= 4.184J（熱化学）

= 4.1855J（15℃）

= 4.1868J（国際蒸気表）

仕事率　1 PS(仏馬力)

= 75 kgf·m/s

= 735.499W

放射能

Bq	Ci
1	2.70270×10^{-11}
3.7×10^{10}	1

吸収線量

Gy	rad
1	100
0.01	1

照射線量

C/kg	R
1	3876
2.58×10^{-4}	1

線量当量

Sv	rem
1	100
0.01	1

（86年12月26日現在）